Available online at www.sciencedirect.com
ScienceDirect
Journal of Sound and Vibration 309 (2008) 823–837
JOURNAL OF SOUND AND VIBRATION
www.elsevier.com/locate/jsvi

On the dynamic behaviour of a mass supported by a parallel combination of a spring and an elastically connected damper

M.J. Brennan[a,*], A. Carrella[a], T.P. Waters[a], Vicente Lopes Jr.[b]

[a]*Institute of Sound and Vibration Research, University of Southampton, Southampton, Hampshire SO17 1BJ, UK*
[b]*Department of Mechanical Engineering, Universidade Estadual Paulista—UNESP/Ilha Solteira, Av. Brasil, 5385-000 Ilha Solteira, SP, Brazil*

Received 14 October 2006; received in revised form 29 July 2007; accepted 30 July 2007
Available online 30 October 2007

Abstract

This paper presents a consistent and concise analysis of the free and forced vibration of a mass supported by a parallel combination of a spring and an elastically supported damper (a Zener model). The results are presented in a compact form and the physical behaviour of the system is emphasised. This system is very similar to the conventional single-degree-of freedom system (sdof)—(Voigt model), but the dynamics can be quite different depending on the system parameters. The usefulness of the additional spring in series with the damper is investigated, and optimum damping values for the system subject to different types of excitation are determined and compared.

There are three roots to the characteristic equation for the Zener model; two are complex conjugates and the third is purely real. It is shown that it is not possible to achieve critical damping of the complex roots unless the additional stiffness is at least eight times that of the main spring. For a harmonically excited system, there are some possible advantages in using the additional spring when the transmitted force to the base is of interest, but when the displacement response of the system is of interest then the benefits are marginal. It is shown that the additional spring affords no advantages when the system is excited by white noise.

1. Introduction

The classic mass–spring–damper single degree-of-freedom (sdof) system is the bedrock of vibration analysis and has been studied at length over many decades. Any elementary textbook on vibration analysis describes the free and forced vibration of a sdof system in detail. In the context of vibration isolation, where the parallel combination of the spring and damper are representative of the isolation system, the damper performs a useful function at the resonance frequency of the system, but is detrimental at high frequencies. It has therefore been suggested that elastically connecting the spring may offer some potential benefits [1]. A thorough investigation of the modified sdof has been conducted and is described comprehensively in Ref. [2].

*Corresponding author.
E-mail address: mjb@isvr.soton.ac.uk (M.J. Brennan).

0022-460X/$ - see front matter © 2007 Elsevier Ltd. All rights reserved.
doi:10.1016/j.jsv.2007.07.074

Combinations of springs and dampers are of interest to the materials community as they are used to represent the behaviour of viscoelastic materials [3]. The parallel combination of a spring and a mass is generally called the *Voigt* model, the series combination of a spring and a damper is called the *Maxwell* model and the parallel combination of a spring and an elastically supported damper is called the *Zener* model. These terms are used in this paper for such systems supporting a mass.

Free vibration of the Zener model was studied by Yamakawa [4]. Muller [5] also studied this model, some 44 years later, in terms of parameters more concerned with material properties such as "*relaxation time*". He also showed that the characteristic equation of the system comprises three roots, one of which is purely real and the other two being complex conjugates. His analysis demonstrated that the complex roots become real under certain situations. However, his approach was such that his explanation of this phenomenon was mathematical rather than physical. Muravyov and Hutton [6] have studied a system similar to the Zener model, where a mass is suspended by a parallel combination of a viscoelastic spring and a viscous dashpot. They showed that over- or under-damped oscillations occur depending on the parameters of the viscoelastic spring.

Because the Zener model is of interest in vibration isolation and in material characterisation it is perhaps surprising that the literature offers little other work on this subject other than the aforementioned references. It is worth noting that there is not a consistent reference trail from the later to the earlier papers. The present paper hopes to contribute by analysing the free and forced vibration of the Zener model in a consistent manner and presenting the results in a compact form with particular emphasis on the physical behaviour of the system.

Optimum damping values for various stated criteria for each of the situations (free vibration, harmonic excitation and white noise excitation) are derived for each case, and are compared. For forced vibration, the amplitude response of the mass is considered, as is the force transmitted to the rigid base.

2. Free vibration

The sdof system shown in Fig. 1 consists of a mass, m, supported by a parallel combination of a spring, k, and an elastically attached viscous damper, c, where the connecting spring has stiffness Nk ($N \geqslant 0$). The spring in series with the dashpot is referred to as the *secondary spring* as opposed to the *primary spring* which is the one in parallel with the damper. This system is commonly referred to as the Zener model, and its equation of

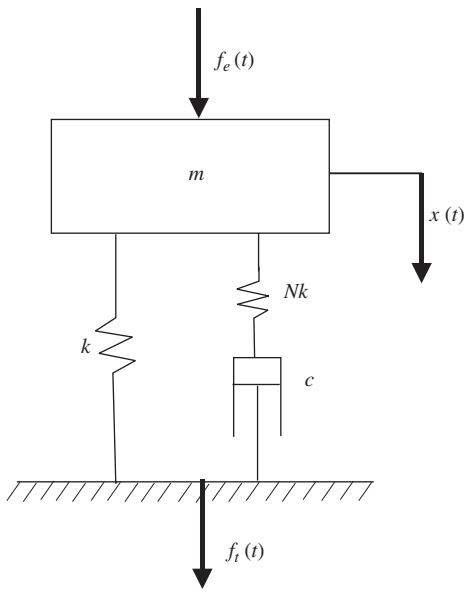

Fig. 1. A point mass supported on a parallel combination of a spring and an elastically attached viscous damper (Zener model).

motion of free vibration is given by [1,2]

$$\left(\frac{mc}{Nk}\right)\dddot{x} + m\ddot{x} + c\left(\frac{N+1}{N}\right)\dot{x} + kx = 0. \tag{1}$$

Eq. (1) can be written in terms of the non-dimensional damping coefficient $\varsigma = c/2\sqrt{mk}$ and the undamped natural frequency of the system when $N = 0$, $\omega_0 = \sqrt{k/m}$, as

$$\left(\frac{2\varsigma}{\omega_0 N}\right)\dddot{x} + \ddot{x} + 2\varsigma\omega_0\left(\frac{N+1}{N}\right)\dot{x} + \omega_0^2 x = 0. \tag{2}$$

Note that $\varsigma = c/2\sqrt{mk}$ is a convenient non-dimensional damping parameter and *not* the damping ratio of the system. As such, the usual symbol for damping ratio, ζ, has been deliberately avoided. Eq. (2) is a third-order differential equation with solutions of the form

$$x(t) = Ae^{s_1 t} + Be^{s_2 t} + Ce^{s_3 t}, \tag{3}$$

where A, B, C are constants that depend on the initial conditions and s_1, s_2, s_3 are the solutions of the system's characteristic equation

$$\left(\frac{2\varsigma}{\omega_0 N}\right)s^3 + s^2 + 2\varsigma\omega_0\left(\frac{N+1}{N}\right)s + \omega_0^2 = 0. \tag{4}$$

Alternatively, a non-dimensional form of the solution can be assumed

$$x(t) = Ae^{\hat{s}_1\tau} + Be^{\hat{s}_2\tau} + Ce^{\hat{s}_3\tau}, \tag{5}$$

where $\hat{s}_i = s_i/\omega_0$ and $\tau = \omega_0 t$ is non-dimensional time. The characteristic equation can then be written as

$$\hat{s}^3 + \left(\frac{N}{2\varsigma}\right)\hat{s}^2 + (N+1)\hat{s} + \left(\frac{N}{2\varsigma}\right) = 0. \tag{6}$$

The three roots of this equation are either all real, or include a complex conjugate pair that characterises under-damped motion [5]. The roots of this equation are given in Appendix A. To determine when critical damping occurs, the imaginary parts of the roots of Eq. (6) are set to zero and solved for ς. The algebraic steps for this procedure can also be found in Appendix A. For a given stiffness ratio N, the values of ς for which this can occur are found to be

$$\varsigma = N\frac{\sqrt{2}}{8}\sqrt{\frac{N^2+20N-8}{(N+1)^3} \pm \frac{\sqrt{N(N-8)^3}}{(N+1)^3}}. \tag{7}$$

There are no real solutions to Eq. (7) when $N<8$ which means that critical damping cannot be achieved if the secondary spring is too soft. This is illustrated by the root locus in Fig. 2(a) in which the roots have been calculated for $0.001 \leqslant \varsigma \leqslant 20$ in increments of 0.05. When $\varsigma = 0$ (no damping) the complex roots are purely imaginary with $\hat{s}_{2,3} = \pm j$, and the system becomes a mass supported on the primary spring alone. As the damper coefficient is increased the complex conjugate pair of roots move in the direction of the arrows and become under-damped. The damped natural frequency is given by the imaginary part of the roots. Further increases in damping coefficient results in a reduction in the real part of the roots and hence the damping in the system. In the limit as $\varsigma \to \infty$ the damper acts as a rigid link and the system collapses to a mass supported on the primary and secondary springs in parallel, i.e. an undamped system. The natural frequency is $\sqrt{N+1}$ times that of the original undamped system, when $\varsigma = 0$. When $\varsigma \ll 1$ the real root $\hat{s}_1$ is very large and negative, and as ς increases the real root moves towards the origin.

When $N>8$ there are two values of ς that satisfy Eq. (7). These solutions are distinct critical damping coefficients for the complex roots of the system, ς_{lower} and ς_{upper} say. When $N \gg 8$, then $\varsigma_{\text{lower}} \approx 1$, the system is critically damped for approximately the same value of damping coefficient as the corresponding Voigt model. The upper value $\varsigma_{\text{upper}} \approx \sqrt{N}/4$ corresponds to a larger value of damping coefficient that also yields critical damping. Taking $N = 15$ as an example, Fig. 2(b) illustrates the root locus when $N>8$. Again, the complex conjugate pair of roots is purely imaginary when $\varsigma = 0$, and initially become increasingly damped as ς

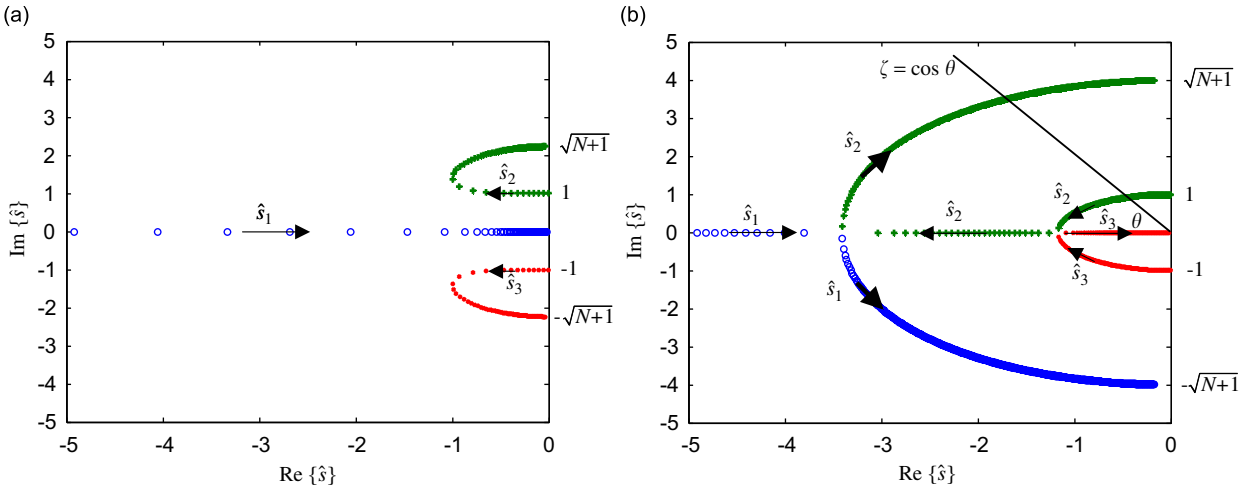

Fig. 2. Examples of the solutions to the characteristic equation of the Zener model as ς is increased from 0.001 to 20 in increments of 0.005: (a) root loci for $N=4$. (b) Root loci for $N=15$.

increases. When $\varsigma=\varsigma_{\text{lower}}$ the root pair become real, one becoming increasingly negative and one moving towards the origin. The root that is real when $\varsigma\ll 1$, ($\hat{s}_1$), is initially large and negative, and moves towards the origin as ς increases. When $\varsigma=\varsigma_{\text{upper}}$ this root and the root moving towards the left on the real axis, ($\hat{s}_2$), become complex; they become less damped as ς increases further until there is effectively zero damping in the system as in the previous case.

In a sdof system, where the mass is supported on a parallel combination of a spring and damper (Voigt model), the governing equation of motion has two roots. These roots are complex when the damping ratio is less than one and are real when the damping ratio is greater than one. The damping ratio of the system is defined by $-\text{Re}\{\hat{s}_{1,2}\}/|\hat{s}_{1,2}|$ [7]. In a system where the dashpot is elastically supported, the damping of the system cannot be uniquely defined because when $\varsigma<\varsigma_{\text{lower}}$ and $\varsigma_{\text{upper}}<\varsigma$ there are always two complex roots and one real root. However, the damping ratios corresponding to the complex roots can be defined in a similar way to the Voigt model [8]. For each value of ς, the damping ratio for these roots is given by

$$\zeta=\cos\theta=\frac{-\text{Re}\{\hat{s}_{1,2}\}}{|\hat{s}_{1,2}|}. \tag{8}$$

This is illustrated in Fig. 2(b). It can be seen that there are two roots that have the same angle θ. Thus, the same damping ratio ζ is obtained for two different values of ς, and for each N there are two values of damping ratio for each oscillatory root. This is shown in the contour plot of Fig. 3(a) for $0\leqslant N\leqslant 30$ and $0\leqslant\varsigma\leqslant 3$. Also plotted in Fig. 3(a) are the lines given by Eq. (7a,b). The region enclosed by the two curves represents combined values of N and ς that result in over-damped motion.

The damped natural frequency normalised by ω_0 is plotted in Fig. 3(b). When $N<8$, the damped natural frequency either increases or decreases first then increases as ς increases. However, when $N\geqslant 8$, the damped natural frequency first decreases as ς increases, and then it increases again. This can also be seen in Fig. 3(b).

Of practical interest is the maximum damping that can be achieved for a given N when $N\leqslant 8$. The form of Eq. (6) is the same as that in Ref. [9], which describes integrated force feedback control of a truss structure. In Ref. [9], an expression is given for the maximum possible damping ratio of the system. This can be adapted to the Zener model, which results in a maximum possible damping coefficient for $N\leqslant 8$, of

$$\zeta_{\max}=\frac{\sqrt{N+1}-1}{2}. \tag{9}$$

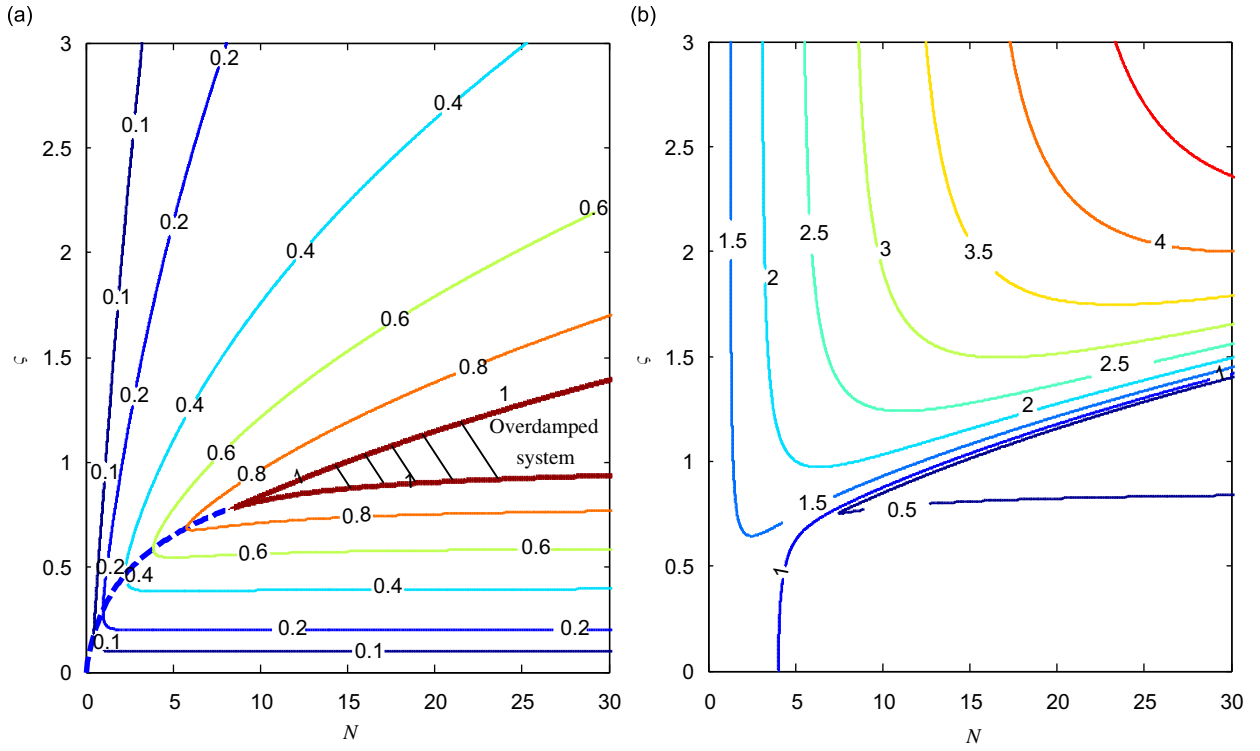

Fig. 3. Dynamic characteristics of free vibration of the Zener model: (a) Contour plot showing the damping ratio of roots $\hat{s}_{1,2}$. The dashed line shows the maximum damping ratio for $N<8$. (b) Contour plot showing the damped natural frequency normalised by ω_0.

The corresponding value of ς is determined by setting

$$\frac{\mathrm{Re}\{\hat{s}_{1,2}\}}{|\hat{s}_{1,2}|} = \frac{\sqrt{N+1}-1}{2} \tag{10}$$

and solving for ς, which results in

$$\varsigma = \frac{N}{2(N+1)^{3/4}}, \quad N \leqslant 8. \tag{11}$$

This is also plotted in Fig. 3(a) as a dashed line. The minimum real part of the underdamped root for the case when $N \leqslant 8$ is given by

$$\mathrm{Re}(\hat{s})\big|_{\min} = \frac{N}{4} \tag{12}$$

and this occurs when

$$\varsigma = \frac{N}{N+2}. \tag{13}$$

In Fig. 4, part of the root locus of $\hat{s}_2$ when $N = 4$ is plotted. Also plotted is the root locus of a second order system with an undamped natural frequency normalised by ω_0 of $(1+\sqrt{N+1})/2$. The tangent to the root locus of $\hat{s}_2$ drawn from the origin intersects *with* the root locus of the second-order system *and* the line $N/4$. Thus, the maximum damping ratio can be interpreted as the damping ratio for an equivalent second order system, which has an undamped natural frequency of $\omega_n/\omega_0 = (1+\sqrt{N+1})/2$ and a root to its normalised characteristic equation that has a real part equal to $-N/4$.

To illustrate the effect of the purely real root on the free vibration of the Zener model, two simulations are presented in Figs. 5(a) and (b). The first is the normalised impulse response of the system, $x(t)/(\hat{f}/m\omega_d)$, where

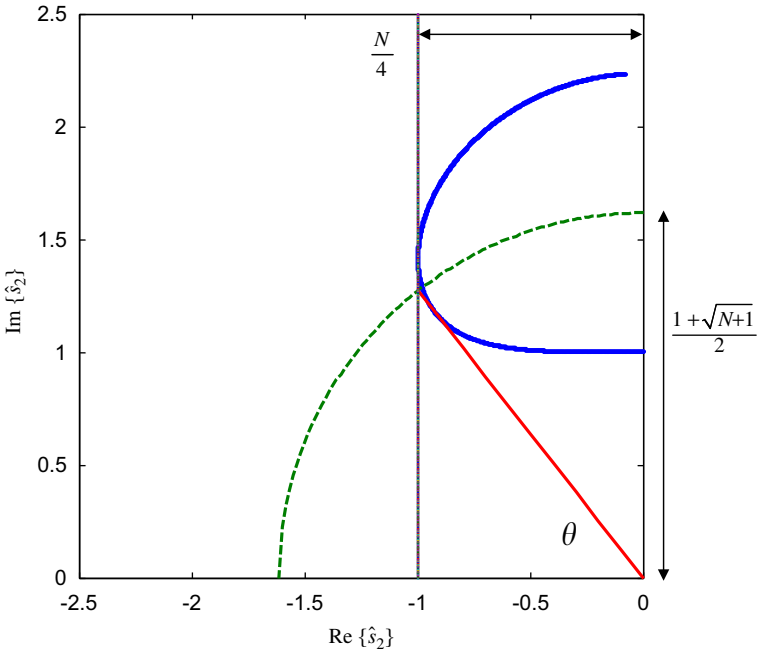

Fig. 4. Graph showing part the root locus of $\hat{s}_2$ when $N = 4$. The solid line is the root locus and the dashed line is the root locus of a second order system with an undamped natural frequency normalised by ω_0 of $(1 + \sqrt{N+1})/2$.

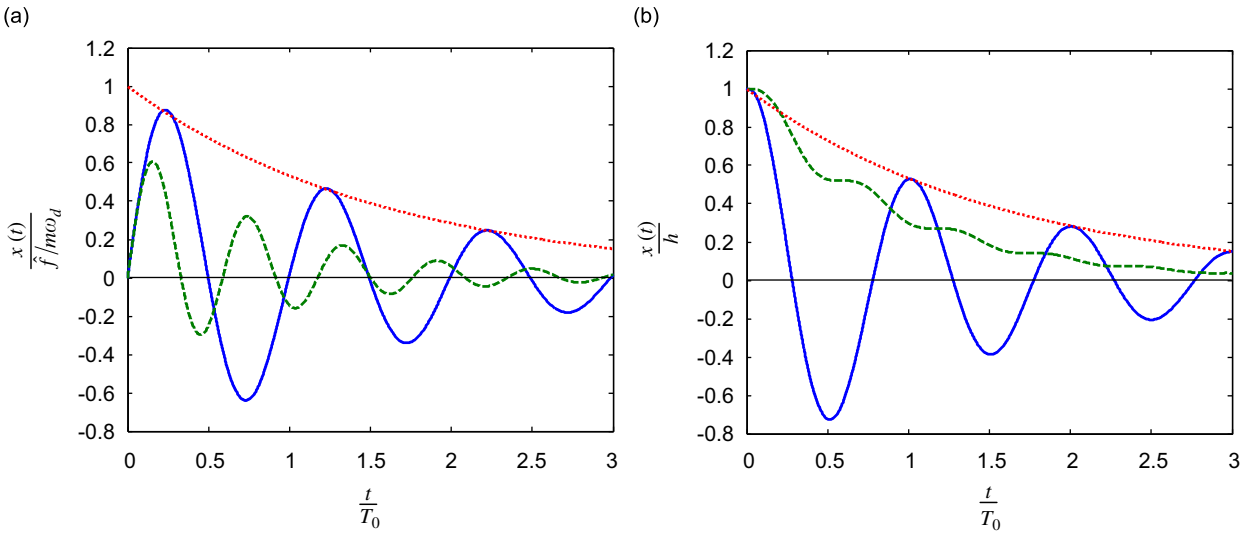

Fig. 5. Free vibration of the Zener model for two different initial conditions. $N = 2$ and $\varsigma = 0.1$: (a) Impulse response of the Zener system. Solid line, $\varsigma = 0.1$; dashed line, $\varsigma = 1.92$; dotted line, $\exp(-\zeta\omega_0 t)$. (b) Response of the Zener model to an initial displacement h. Solid line, $\varsigma = 0.1$; dashed line, $\varsigma = 1.92$; dotted line, $\exp(-\zeta\omega_0 t)$.

$\hat{f}$ is a unit impulse and ω_d is the damped natural frequency, and the second is the normalised response to a displacement input $x(t)/h$, where h is the initial displacement. Both responses are plotted as a function of non-dimensional time t/T_0 where $T_0 = 2\pi/\omega_0$ is the undamped natural period of the system when $N = 0$. To determine the constants in Eq. (5), the following equations have to be solved for the impulse response and the

displacement input response, respectively:

$$\begin{bmatrix} A \\ B \\ C \end{bmatrix} = \begin{bmatrix} 1 & 1 & 1 \\ \hat{s}_1 & \hat{s}_2 & \hat{s}_3 \\ \hat{s}_1^2 & \hat{s}_2^2 & \hat{s}_3^2 \end{bmatrix}^{-1} \begin{bmatrix} 0 \\ 1 \\ 0 \end{bmatrix} \quad \text{and} \quad \begin{bmatrix} A \\ B \\ C \end{bmatrix} = \begin{bmatrix} 1 & 1 & 1 \\ \hat{s}_1 & \hat{s}_2 & \hat{s}_3 \\ \hat{s}_1^2 & \hat{s}_2^2 & \hat{s}_3^2 \end{bmatrix}^{-1} \begin{bmatrix} 1 \\ 0 \\ 0 \end{bmatrix}. \tag{14a,b}$$

The values of $\hat{s}_i$ are determined numerically by solving Eq. (6) for $N = 2$ and $\varsigma = 0.1$ and 1.92 (which correspond to a value of $\zeta = 0.1$).

The main difference between the Zener and the Voigt models is the additional purely real root. This root is large and negative (−9.8) when $\varsigma = 0.1$ and small and negative (−0.18) when $\varsigma = 1.92$. The effects of this root on the free response can be observed in Figs. 5(a) and (b). It can be seen that the real root has a negligible effect when $\varsigma = 0.1$ as both the impulse response and the displacement input response are similar to that of the Voigt model and are thus dominated by the complex roots. However, when $\varsigma = 1.92$ the effect of the purely real root on the response is very much dependent on the initial conditions. For the impulse response, the complex roots dominate the response, but for the displacement input it is clear that the purely real root dominates the response.

As noted by Muller [5], because there is always one purely real root, the characteristic Eq. (6) can be written as

$$(\hat{s} + s_0)(\hat{s}^2 + a\hat{s} + b) = 0, \tag{15}$$

where s_0, a and b can be determined by comparing Eqs. (6) and (15). In general, Eq. (15) has a complicated form from which little new knowledge can be gained. However, there are two situations when the characteristic equation can be factorised easily, which is when

$\varsigma \ll N$. In which case Eq. (6) becomes

$$(\hat{s} + \varsigma + j)(\hat{s} + \varsigma - j)\left(\hat{s} + \frac{N}{2\varsigma}\right) = 0. \tag{16a}$$

$\varsigma \gg N$. In which case Eq. (6) becomes

$$\left(\hat{s} + \frac{N^2}{4(1+N)\varsigma} + j\sqrt{N+1}\right)\left(\hat{s} + \frac{N^2}{4(1+N)\varsigma} - j\sqrt{N+1}\right)\left(\hat{s} + \frac{N}{2(1+N)\varsigma}\right) = 0. \tag{16b}$$

The magnitudes of the real parts of the roots of the characteristic equation, which govern the decay of free vibration, are calculated numerically for $N = 4$ and plotted in Fig. 6 (all are negative) as a function of ς.

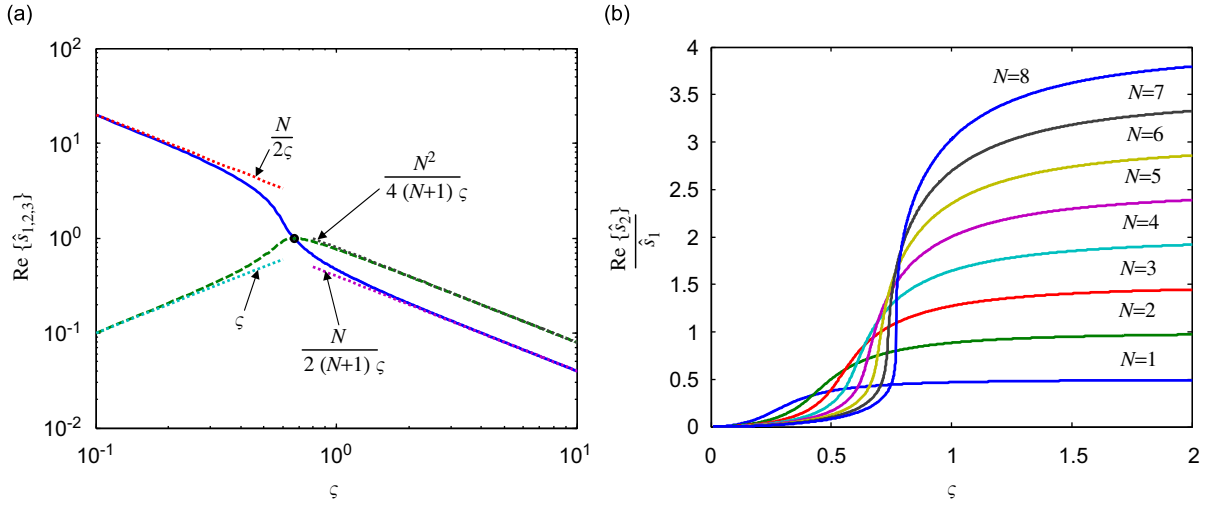

Fig. 6. Graphs to show the behaviour of the real parts of the roots for the Zener model as ς increases: (a) Magnitudes of the real part of the roots when $N = 4$ as ς increases (they are all negative). The dotted lines show the asymptotic behaviour. The roots are equal (°) when $\varsigma = N/(6\sqrt{N/2-1})$. (b) The ratio of $\mathrm{Re}\{\hat{s}_2\}/\hat{s}_1$ plotted as a function of ς for different values of N. $\mathrm{Re}\{\hat{s}_2\}/\hat{s}_1 \approx N/2$ when $\varsigma \gg 1$.

The real parts of the roots of Eq. (16a) and (16b) are also plotted. It can be seen that they are the asymptotes for the real parts of the roots when $\varsigma \ll 1$ and $\varsigma \gg N$. It can also be seen that the purely real root is much larger than the real part of the complex roots when $\varsigma \ll 1$, but when $\varsigma \gg 1$ the real part of the complex roots is greater than the purely real root. When the real part of the complex roots is equal to the purely real root, then

$$\varsigma = \frac{N}{6\sqrt{N/2-1}}. \tag{17}$$

The ratio of the real parts of the roots is plotted as a function of ς in Fig. 6(b) for different values of N. It can be seen in Figs. 6(a) and (b) that when $\varsigma \gg 1$ then $\mathrm{Re}\{\hat{s}_2\}/\hat{s}_1 \approx N/2$. Note that this is only a function of N.

Generally, the root with the smallest real part dominates the decay of free vibration, thus Eqs. (16a) and (16b) can be used to obtain analytical expressions for the free response of the Zener model in certain situations.

3. Forced vibration

This section is concerned with the forced response of the Zener model. Two situations are considered; the first is harmonic excitation and is described in Section 3.1, and the second is for white noise excitation and is discussed in Section 3.2.

3.1. Harmonic excitation

The dynamic response of the Zener model to forced *harmonic* excitation has been reported comprehensively in the literature, for example [1,2]. Therefore, only the key results are presented here, but in a way that is consistent with the results for free vibration discussed in Section 2. Two responses are considered; the non-dimensional displacement response of the system or the *dynamic magnification factor* given by $D(j\Omega) = X/(F_e/k)$, where $\Omega = \omega/\omega_0$, and the ratio of the transmitted force F_t to the excitation force F_e, or the *transmissibility* given by $T(j\Omega) = F_t/F_e$. These can be derived from Eq. (2) in a straightforward manner by assuming a harmonic excitation force $F_e e^{j\omega t}$. The dynamic magnification factor is given by

$$D(j\Omega) = \frac{1 + j(2/N)\varsigma\Omega}{1 - \Omega^2 + j(2/N)\varsigma\Omega(N + 1 - \Omega^2)}. \tag{18}$$

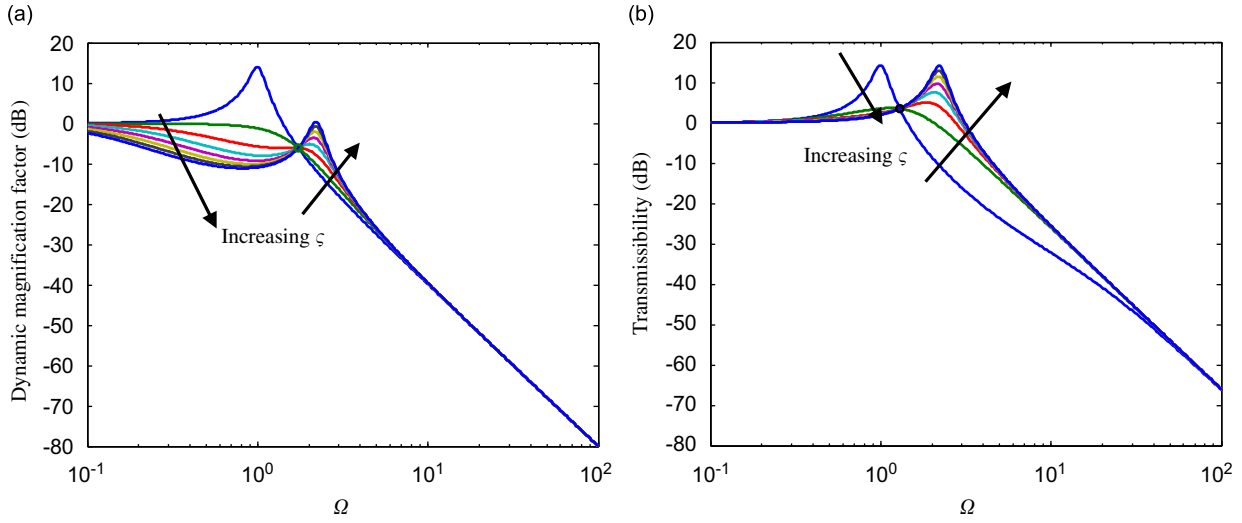

Fig. 7. Forced harmonic vibration response of the Zener model (dynamic magnification factor and transmissibility) for $N = 4$ as ς varies from 0.1 to 4 in steps of 0.5: (a) Magnitude of the dynamic magnification factor for the Zener model. (b) Magnitude of the transmissibility for the Zener model.

The modulus is plotted in Fig. 7(a) for values of ς from 0.1 to 4 in steps of 0.5. It can be seen that the resonance peak reduces initially as ς increases, and then it increases again, but with the peak occurring at a higher frequency. In the limit when $\varsigma \to 0$, $\Omega \to 1$, and when $\varsigma \to \infty$, $\Omega \to \sqrt{N+1}$. The modulus passes through the point $|X/(F_e/k)| = 2/N$ [1], for *all* values of ς, which is marked by $^\circ$ in Fig. 7(a). This occurs when the non-dimensional frequency $\Omega = \sqrt{(N+2)/2}$. The peak in the dynamic magnification factor is a minimum at this frequency, when the non-dimensional damping coefficient is [1]

$$\varsigma = \frac{N}{\sqrt{2(N+2)}}. \tag{19}$$

The damping value given by Eq. (19) is referred to as *optimum damping* in the literature as it yields the smallest displacement response at resonance. From the above discussion, it can be seen that the magnitude of the peak in the dynamic magnification factor is a function of N and ς. To compare the forced response of the Zener model with the free vibration characteristics depicted in Fig. 3, the *reciprocal* of the peak value is plotted as a contour graph as a function of N and ς in Fig. 8(a); Eq. (19) is also plotted for comparison. The peak in the dynamic magnification factor can only be less than unity when $N > 2$. It can be seen that for $N > 2$ and for ς less than about 0.3, the reciprocal of the peak value $\approx 2\varsigma$. Thus, the relationship between the damping of the complex roots and the non-dimensional damping coefficient is $\zeta \approx \varsigma$.

Inspection of Fig. 8(a) also shows that there is a wide range of values of ς for a given N greater than about 2 that results in the system having a maximum dynamic magnification factor of one. This does not occur at a resonance frequency, however, but at zero frequency as can be seen in Fig. 7(a). This can also be seen in Fig. 8(b), which shows the contour plot of the normalised frequency at which the *maximum* value of the dynamic magnification factor. When $N \gg 1$ the frequency at which the peak occurs decreases as ς increases (as it would in the Voigt model), until $\varsigma = 1/\sqrt{2}$ when $\Omega = 0$. For low values of N the situation is quite different. For ς greater than about $1/\sqrt{2}$, as N increases the frequency at which the peak occurs also increases. The peak value, however, decreases as can be seen in Fig. 8(a), and when it decreases below unity, the maximum value occurs when $\Omega = 0$. The line marked "all contours" gives the values of N and ς when the peak value just dips below unity.

Further insight can be gained by examining the *transfer* function of the system rather than the frequency response function. This is given by

$$D(\hat{s}) = \frac{\hat{s} + (N/2\varsigma)}{\hat{s}^3 + (N/2\varsigma)\hat{s}^2 + (N+1)\hat{s} + (N/2\varsigma)}. \tag{20}$$

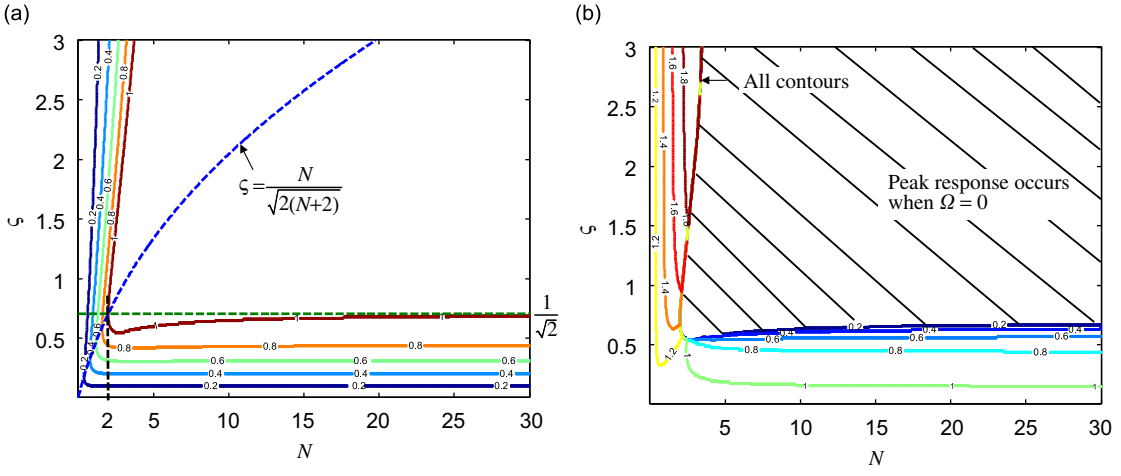

Fig. 8. Forced harmonic vibration response of the Zener model (dynamic magnification factor): (a) Contour plot showing the *reciprocal* of the maximum value of the dynamic magnification factor. The dashed line $\varsigma = N/\sqrt{2(N+2)}$ results in a minimum peak. (b) Contour plot showing the frequency normalised by ω_0 at which the maximum of the dynamic magnification factor.

When $\varsigma \ll N$, the denominator factorises as in Eq. (16a), and Eq. (18) reduces to

$$D(\hat{s}) \approx \frac{1}{(\hat{s}+\varsigma+j)(\hat{s}+\varsigma-j)}, \tag{21}$$

which means that for the frequency response function, the effect of the real root is effectively cancelled by the zero, which is given by $-N/(2\varsigma)$ (found be setting the numerator to zero and solving for $\hat{s}$). Thus, the oscillatory roots dominate the response for all frequencies.

If $\varsigma \gg N$, Eq. (20) can be written as

$$D(\hat{s}) \approx \frac{\hat{s}+(N/2\varsigma)}{\left(\hat{s}+\dfrac{N^2}{4(N+1)\varsigma}+j\sqrt{N+1}\right)\left(\hat{s}+\dfrac{N^2}{4(N+1)\varsigma}-j\sqrt{N+1}\right)\left(\hat{s}+\dfrac{N}{2(N+1)\varsigma}\right)}. \tag{22}$$

It can be seen that in this case the numerator does not cancel with the purely real root as it does when $\varsigma \ll N$ as discussed above. Thus, if the damping is high the purely real root cannot be neglected as it plays a role in the frequency response of the system. However, at high frequencies $|D(j\Omega)| \approx 1/\Omega^2$ as can be seen by inspecting Eq. (22) and Fig. 7(a).

Examination of Fig. 8(a) shows that there seems to be a marginal advantage in using an elastically supported damper because for small values of N the normalised peak response can be limited to unity for a smaller damping coefficient compared to the Voigt model.

A parameter that characterises the performance of an isolator is its Transmissibility, which, for an isolator described by the Zener model, is given by

$$T(j\Omega) = \frac{F_t}{F_e} = \frac{1+j(2/N)(N+1)\varsigma\Omega}{1-\Omega^2+j(2/N)\varsigma\Omega(N+1-\Omega^2)}. \tag{23}$$

It can be seen that Eq. (23) is identical to Eq. (18) except for the additional term $(N+1)$ in the numerator. The modulus of the Transmissibility is plotted in Fig. 7(b) for values of ς from 0.1 to 4 in steps of 0.5. As with the dynamic magnification factor, the resonant peak reduces initially as ς increases, and then it increases again but with the peak occurring at a higher frequency. It has the same frequency limits as $\varsigma \to 0$ and $\varsigma \to \infty$ as with the dynamic magnification factor. The modulus passes through the point $|T(j\Omega)| = (N+2)/N$ [1], for *all* values of ς, which is marked by $^\circ$ in Fig. 7(b). This occurs when the non-dimensional frequency $\Omega = \sqrt{2(N+1)/(N+2)}$. The peak in the transmissibility is a minimum at this frequency, when the

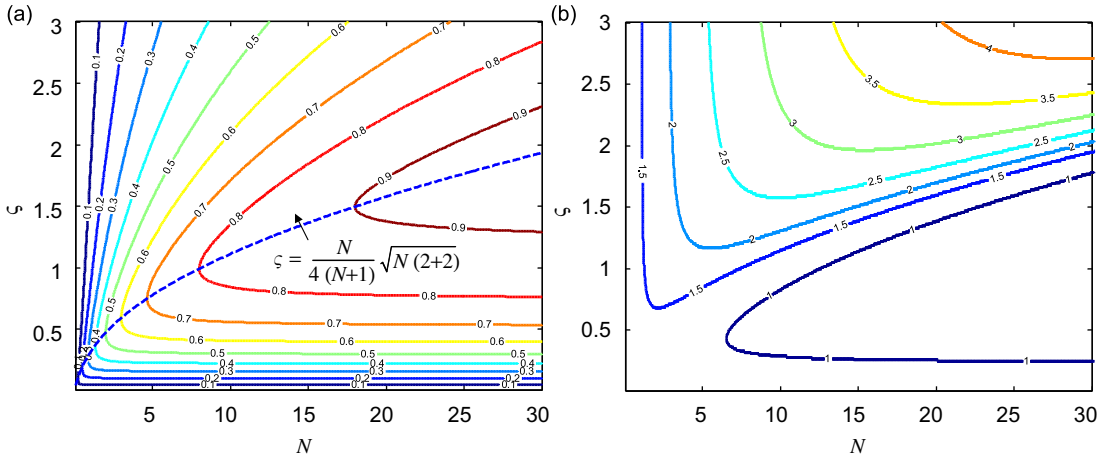

Fig. 9. Forced harmonic vibration of the Zener model (transmissibility): (a) Contour plot showing the *reciprocal* of the maximum value of the transmissibility. The dashed line shows the value of ς those results in a minimum peak. (b) Contour plot showing the frequency normalised by ω_0 at which the peak response of the transmissibility occurs.

non-dimensional damping coefficient is [1]

$$\varsigma = \frac{N}{4(N+1)}\sqrt{2(N+2)}. \tag{24}$$

The damping value given by Eq. (24) is referred to as *optimum damping* in the literature as it yields the lowest transmissibility at resonance.

The contour plots for the *reciprocal* of the maximum value of the transmissibility and the non-dimensional frequency at which this occurs are plotted in Figs. 9(a) and (b), respectively. Eq. (23) is also plotted for comparison in Fig. 9(a). These figures can be compared with the corresponding contour plots for the dynamic magnification factor in Fig. 7. It can be seen that there are significant differences. For a wide range of system parameters, the peak in the dynamic magnification factor was unity when the frequency was zero. This is not so with the Transmissibility; only if $N \gg 1$ and $\varsigma \gg 1$ does the maximum occur at zero frequency. One notable feature in Fig. 9, is that the natural frequency changes rapidly with ς in the region where the damping has been optimised according to Eq. (24).

The *transfer* function of the transmissibility is given by

$$T(\hat{s}) = \frac{(N+1)\left(\hat{s} + \left(\dfrac{N}{2\varsigma(N+1)}\right)\right)}{\hat{s}^3 + \left(\dfrac{N}{2\varsigma}\right)\hat{s}^2 + (N+1)\hat{s} + \left(\dfrac{N}{2\varsigma}\right)}. \tag{25}$$

When $\varsigma \ll N$, the denominator factorises as in Eq. (16a), and Eq. (25) reduces to

$$T(\hat{s}) \approx \frac{(N+1)\left(\hat{s} + \left(\dfrac{N}{2\varsigma(N+1)}\right)\right)}{(\hat{s}+\varsigma+j)(\hat{s}+\varsigma-j)\left(\hat{s} + \dfrac{N}{2\varsigma}\right)}. \tag{26}$$

It can be seen that unless $N \ll 1$ the purely real root in the denominator does not cancel with the zero, and so all three roots of the characteristic equation influence the frequency response function. This is different to dynamic magnification factor discussed above. At high frequencies, the transmissibility is given by $|T(j\Omega)| \approx (N+1)/\Omega^2$, i.e., independent of ς, and rolls off at 40 dB/decade. Conversely, for a system with a rigidly connected damper the high frequency transmissibility is $|T(j\Omega)| \approx \varsigma/\Omega$ and presents a decay slope of 20 dB/decade. It can be concluded that the Zener model out-performs the conventional system at high frequencies, i.e. when $\Omega > 1/\varsigma(N+1)$.

3.2. White noise excitation

Many systems are excited by random rather than harmonic vibration. To make the analysis tractable, white-noise excitation is considered. As with harmonic excitation, both the dynamic magnification factor and transmissibility are considered for the Zener model.

The mean square displacement response is given by [10]

$$\bar{x}^2 = S_0 \int_0^\infty |D(j\Omega)|^2 \, \mathrm{d}\Omega, \tag{27}$$

where S_0 is the amplitude of the excitation spectral density. Substituting for $D(j\Omega)$ from Eq. (18) into Eq. (27) and evaluating the integral gives, in non-dimensional form

$$\frac{\bar{x}^2}{S_0\omega_0\pi/4} = \frac{1}{\varsigma} + \frac{4\varsigma}{N^2}. \tag{28}$$

When $\varsigma \ll N$

$$\frac{\bar{x}^2}{S_0\omega_0\pi/4} \approx \frac{1}{\varsigma}. \tag{29a}$$

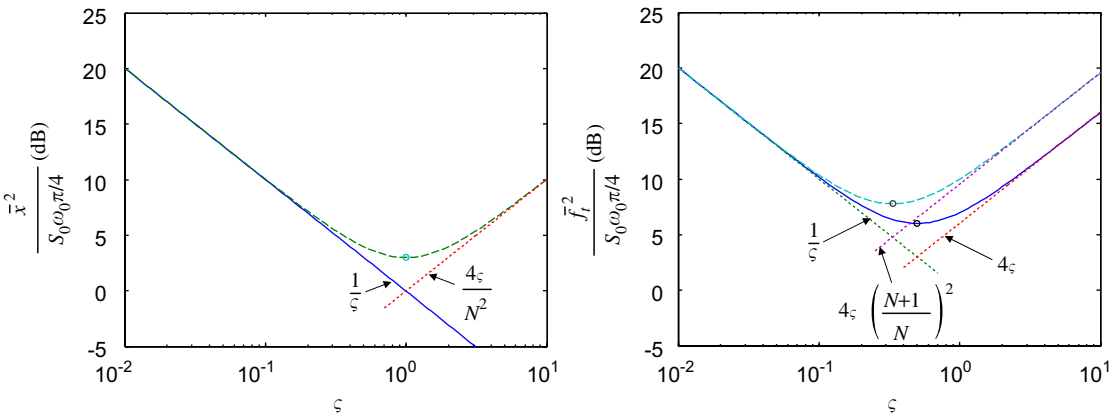

Fig. 10. Normalised mean square responses of the Zener model for white noise excitation: (a) Normalised mean square displacement response of the mass. Solid line, the displacement response when $N\to\infty$, dashed line for $N=2$. (b) Transmitted force. Solid line, the transmitted force when $N\to\infty$, dashed line for $N=2$.

When $\varsigma \gg N$

$$\frac{\bar{x}^2}{S_0\omega_0\pi/4} \approx \frac{4\varsigma}{N^2}. \tag{29b}$$

Eq. (29a) is also the normalised displacement response for a sdof system with a rigidly connected damper ($N\to\infty$). Eqs. (28) and (29) are plotted in Fig. 10(a) for $N=2$. It can be seen that the mean square response initially decreases as ς increases, but then increases again. The minimum in the response can be determined by setting the two asymptotes given in Eqs. (29a) and (29b) to be equal. The result is an optimum value of $\varsigma = N/2$ and a minimum normalised mean square response of

$$\left.\frac{\bar{x}^2}{S_0\omega_0\pi/4}\right|_{\min} = \frac{4}{N}. \tag{30}$$

This point is marked as $^\circ$ in Fig. 10(a).

The mean square force transmitted to the base is given by

$$\bar{f}_t^2 = S_0 \int_0^\infty |T(j\Omega)|^2 \, \mathrm{d}\Omega. \tag{31}$$

Substituting for $T(j\Omega)$ from Eq. (23) into Eq. (31) and evaluating the integral gives, in non-dimensional form

$$\frac{\bar{f}_t^2}{(\pi/4)S_0\omega} = \frac{1}{\varsigma} + 4\varsigma\left(\frac{N+1}{N}\right)^2. \tag{32}$$

When $\varsigma \ll N$

$$\frac{\bar{f}_t^2}{S_0\omega_0\pi/4} \approx \frac{1}{\varsigma}. \tag{33a}$$

When $\varsigma \gg N$

$$\frac{\bar{f}_t^2}{S_0\omega_0\pi/4} \approx 4\varsigma\left(\frac{N+1}{N}\right)^2. \tag{33b}$$

If $N\to\infty$ then Eq. (32) reduces to

$$\frac{\bar{f}_t^2}{S_0\omega_0\pi/4} = \frac{1}{\varsigma} + 4\varsigma, \tag{34}$$

which is the normalised mean square force for the system with a rigidly connected damper. Eq. (34) has asymptotes for $\varsigma \ll 1$ of $1/\varsigma$ and for $\varsigma \gg 1$ of ς. Eqs. (32) and (34) are plotted in Fig. 10(b) together with the corresponding asymptotes. It can be seen that, as with the displacement response, the mean square force initially decreases as ς increases, but then increases again. The minimum in the response can be determined by setting the two asymptotes given in Eqs. (33a) and (33b) to be equal. The result is an optimum value of $\varsigma = N/(2(N+1))$ and a minimum normalised mean square response of

$$\left.\frac{\bar{f}_t^2}{S_0\omega\pi/4}\right|_{\min} = \frac{4(N+1)}{N}. \tag{35}$$

If $N \to \infty$, the minimum normalised mean square response is 4 which occurs when $\varsigma = 1/2$. The minima are shown as ϱ in Fig. 10(b). It can be seen that the minimum mean square force for a rigidly connected damper is smaller than that for an elastically connected damper.

4. Discussion

Table 1 summarises the optimum values of the non-dimensional damping coefficient ς_{opt} for free and forced vibrations of the Zener model derived in Sections 2 and 3. These are also plotted in Fig. 11 for comparison. It can be seen that there is not a single optimum value; it depends upon the type of excitation and the response variable of interest. For free vibration, two optima are given, one for $N<8$ and one for $N \geqslant 8$. It has been shown that the complex roots can only be critically damped when $N \geqslant 8$ and this can be achieved with two values of ς. When $N<8$ two of the roots of the characteristic equation are always complex, but there is a value of ς that can achieve maximum damping for these roots. In general, there does not appear to be any advantage in using an elastically connected damper for free or transient vibration, unless there is a particular response that cannot be achieved using a parallel combination of a spring and a damper.

There are two optimum damping values for harmonic excitation, one for the displacement response of the system and one for the force transmitted to the rigid base. Both damping values ensure the response at the resonance frequency is minimised, and have been reported previously in the literature. There seems to be a marginal advantage in using an elastically connected damper if the displacement response is of interest, in that it is possible to achieve critical damping for the system with a smaller damper than in the Voigt model provided that N is chosen carefully. The main advantage is when the transmitted force is of interest. It is possible to have a high-frequency response that decreases with the square of frequency, but with some damping being added to the system to reduce the response at resonance. This is not possible with a rigidly connected damper. However, there is a trade-off between reducing the amplitude of the high-frequency response and reducing the amplitude of the resonance peak. The additional spring in series with the damper gives more flexibility in tuning the system for a particular requirement. It should be noted, however, that the frequency at which the peak occurs is particularly sensitive to the damping coefficient for N greater than about 10.

Table 1
Summary of the optimum non-dimensional damping coefficients ς_{opt} for free and forced vibration of the Zener model

Free vibration		Forced vibration			
$N<8$	$N \geqslant 8$	Harmonic excitation		White noise excitation	
		Dynamic magnification factor	Transmissibility	Mean square displacement response	Mean square transmitted force
$\dfrac{N}{2(N+1)^{3/4}}$	$N\dfrac{\sqrt{2}}{8}\sqrt{\dfrac{N^2+20N-8}{(N+1)^3} \pm \dfrac{\sqrt{N(N-8)^3}}{(N+1)^3}}$	$\dfrac{N}{\sqrt{2(N+2)}}$	$\dfrac{N}{4(N+1)}\sqrt{2(N+2)}$	$\dfrac{N}{2}$	$\dfrac{N}{2(N+1)}$

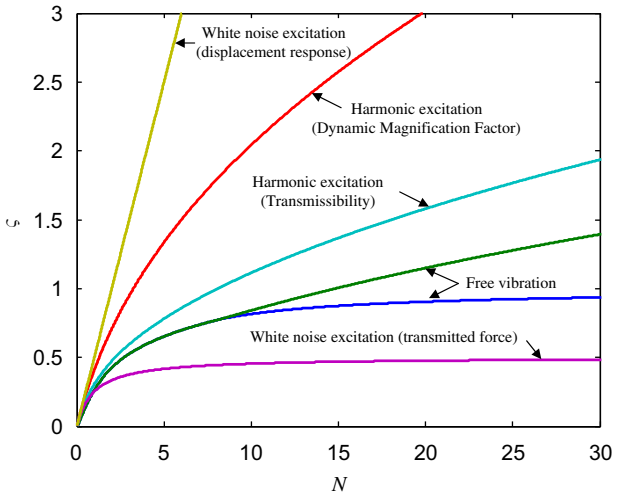

Fig. 11. Optimum values of ς for the Zener model for different excitation conditions.

Examination of Figs. 10(a) and (b) and Table 1 shows that there is no advantage in using an elastically connected damper if the excitation is white noise and the mean square displacement or transmitted force response is of interest. In fact it is detrimental in both cases. If the system is excited by both harmonic and random vibration, then it is possible that an elastically supported damper may offer advantages, but this would have to be considered on a case-by-case basis.

5. Conclusions

This paper has described the free and forced dynamic behaviour of a sdof system in the case where the damper is elastically supported (Zener model). There are three roots to the characteristic equation for this system; two of these are complex conjugates and the third root is purely real. It has been shown that it is not possible to achieve critical damping of the complex roots unless the secondary stiffness is at least eight times that of the primary stiffness. Expressions have been derived for the minimum damping required to critically damp the complex roots when this is possible. Expressions have also been derived for the maximum damping of the complex roots when critical damping is not possible. For comparison and completeness, the behaviour of the system when excited by harmonic vibration has also been presented. It has been shown that there could be some advantages in using a spring in series with a damper when the transmitted force to the base is of interest, but when the displacement response of the system is of interest then the benefits of such a system are marginal. Finally, the response of the Zener model excited by a force that is spectrally white has been considered. Optimum values of the damping have been determined for the cases when the mean square displacement response of the mass, and the mean square force transmitted to the rigid base are of interest. It is shown that the spring in series with the damper affords no advantages, the best situation being when the damper is rigidly connected.

Acknowledgements

The first author would like to acknowledge the support of the Leverhulme Trust for a Study Abroad Fellowship, and also to FAPESP, Brazil.

Appendix A. Solution of the characteristic equation for the Zener model

The closed-form solution of a third-order polynomial equation, which is the form of the characteristic equation for the Zener model given in Eq. (6), was determined in 1545 by Girolamo Cardano [11]. However, in this paper the symbolic algebra software package, Maple [12], was used to determine the roots of Eq. (6),

which is repeated here for convenience:

$$\hat{s}^3 + \left(\frac{N}{2\varsigma}\right)\hat{s}^2 + (N+1)\hat{s} + \left(\frac{N}{2\varsigma}\right) = 0. \tag{A.1}$$

The roots are given by

$$\hat{s}_1 = R_1, \tag{A.2a}$$

$$\hat{s}_{2,3} = R_2 \pm j\frac{\sqrt{3}}{2}Q, \tag{A.2b}$$

where

$$R_1 = \frac{(18\varsigma^2N^2 - 36\varsigma^2N - N^3 + 6\varsigma\sqrt{(3-3\varsigma^2)N^4 + (48\varsigma^4 - 60\varsigma^2)N^3 + (24\varsigma^2 + 144\varsigma^4)N^2 + 144\varsigma^2N + 48\varsigma^4})^{1/3}}{6\varsigma}$$
$$+ \cdots + \frac{N^2 - 12\varsigma^2(N^2+1)}{6\varsigma(18\varsigma^2N^2 - 36\varsigma^2N - N^3 + 6\varsigma\sqrt{(3-3\varsigma^2)N^4 + (48\varsigma^4 - 60\zeta^2)N^3 + (24\varsigma^2 + 144\varsigma^4)N^2 + 144\varsigma^2N + 48\varsigma^4})^{1/3}}$$
$$- \frac{N}{6\varsigma}$$

$$R_2 = -\frac{N^2 - 12\varsigma^2(N^2+1)}{12\varsigma(18\varsigma^2N^2 - 36\varsigma^2N - N^3 + 6\varsigma\sqrt{(3-3\varsigma^2)N^4 + (48\varsigma^4 - 60\varsigma^2)N^3 + (24\varsigma^2 + 144\varsigma^4)N^2 + 144\varsigma^2N + 48\varsigma^4})^{1/3}}$$
$$- \cdots - \frac{N}{6\varsigma},$$

$$Q = \frac{(18\varsigma^2N^2 - 36\varsigma^2N - N^3 + 6\varsigma\sqrt{(3-3\varsigma^2)N^4 + (48\varsigma^4 - 60\varsigma^2)N^3 + (24\varsigma^2 + 144\varsigma^4)N^2 + 144\varsigma^2N + 48\varsigma^4})^{1/3}}{6\zeta}$$
$$- \cdots - \frac{N^2 - 12\zeta^2(N^2+1)}{6\varsigma(18\varsigma^2N^2 - 36\varsigma^2N - N^3 + 6\varsigma\sqrt{(3-3\varsigma^2)N^4 + (48\varsigma^4 - 60\varsigma^2)N^3 + (24\varsigma^2 + 144\varsigma^4)N^2 + 144\varsigma^2N + 48\varsigma^4})^{1/3}}.$$

When there is critical damping the imaginary part of the roots given by Eq. (A.2b) is zero. Thus, by setting $Q = 0$ and rearranging the resulting equation the two positive solutions for ς in terms of N can be determined and are given by

$$\varsigma = N\frac{\sqrt{2}}{8}\sqrt{\frac{N^2 + 20N - 8}{(N+1)^3} \pm \frac{\sqrt{N(N-8)^3}}{(N+1)^3}}. \tag{A.3}$$

References

[1] J.E. Ruzicka, T.E. Derby, *Influence of Damping in Vibration Isolation*, T.S.a.V.I. Centre, US Department of Defense, 1972.

[2] T.F. Derby, P.C. Calcaterra, Response and optimization of an isolator with relaxation type damping, *Shock and Vibration Bulletin* 40 (5) (1970) 203–216.

[3] A.D. Nashif, D.I.G. Jones, J.P. Henderson, *Vibration Damping*, Wiley, New York, 1985.

[4] I. Yamakawa, On the free vibration and the transient state of one-degree-of-freedom system with elastically supported damper, *Bulletin of JSME* 4 (16) (1961) 641–644.

[5] P. Muller, Are the eigensolutions of a 1-d.o.f. system with viscoelastic damping oscillatory or not?, *Journal of Sound and Vibration* 285 (2005) 501–509.

[6] A. Muravyov, S.G. Hutton, Free vibration response characteristic of a simple elasto-hereditary system, *Journal of Vibration and Acoustics—Transactions of the ASME* 120 (1998) 628–632.

[7] B.C. Kuo, *Automatic Control System*, fifth ed., Prentice-Hall International, Englewood Cliffs, NJ, 1987.

[8] S.S. Rao, *Mechanical Vibrations*, second ed., Addison-Wesley, Reading, MA, 1990.

[9] A. Preumont, *Vibration Control of Active Structures*, second ed., Kluwer Academic Publishers, Dordrecht, 2002.

[10] D.E. Newland, *An Introduction to Random Vibrations and Spectral Analysis*, Longman, London, 1975.

[11] G. Cardano, *Ars Magna: The Great Art, or the Rules of Algebra* (translated by R.B. McClenon, in: D.E. Smith (Ed.), *A Source Book in Mathematics*, Dover, New York, 1959, pp. 203–206).

[12] Maplesoft, 615, Kumpf Drive, Waterloo, Ontario, Canada N2V 1KB.